

Testing The Friedmann Equation: The Expansion of the Universe During Big-Bang Nucleosynthesis

Sean M. Carroll¹ and Manoj Kaplinghat²

¹ Department of Physics and Enrico Fermi Institute
The University of Chicago, Chicago, Il 60637, USA
`carroll@theory.uchicago.edu`

² Department of Astronomy and Astrophysics
The University of Chicago, Chicago, Il 60637, USA
`manoj@oddjob.uchicago.edu`

February 1, 2008

Abstract

In conventional general relativity, the expansion rate H of a Robertson-Walker universe is related to the energy density by the Friedmann equation. Aside from the present day, the only epoch at which we can constrain the expansion history in a model-independent way is during Big-Bang Nucleosynthesis (BBN). We consider a simple two-parameter characterization of the behavior of H during BBN and derive constraints on this parameter space, finding that the allowed region of parameter space is essentially one-dimensional. We also study the effects of a large neutrino asymmetry within this framework. Our results provide a simple way to compare an alternative cosmology to the observational requirement of matching the primordial abundances of the light elements.

1 Introduction

Modern cosmology boasts a best-fit model which is in good agreement with a variety of data. This model features a homogeneous and isotropic spatially-flat universe comprised of approximately 5% baryons, 25% cold dark matter, and 70% vacuum energy, with a radiation energy density of about 10^{-4} at a temperature 2.7° K. Along with a nearly scale-free spectrum of adiabatic density perturbations, these ingredients provide an accurate

match to observations of the recent expansion history [1], large-scale structure [2], the cosmic microwave background (CMB) [3], and the abundances of light elements as predicted by Big-Bang Nucleosynthesis (BBN) [4].

As successful as the best-fit model has been, it falls short of achieving an aura of inevitability due to certain problems of naturalness. Foremost among these are the two cosmological constant problems: why the vacuum energy is so small in comparison to its expected value, and why its precise magnitude is so close to that of the matter energy density today [5]. In addition to these unsolved problems, there are problems for which a popular solution exists but is lacking a firm experimental footing: the flatness and horizon problems, which may be solved by inflation, and of course the nature of the dark-matter itself. Finally, amidst the large successes there are small failures of the best-fit model in fitting the data, especially in the detailed matching of structure on small scales to the predictions of cold dark matter [6]. Meanwhile, numerous alternatives to conventional cosmology have been studied. To take one recent example, brane-world models with large extra dimensions can give rise to a variety of departures from four-dimensional general relativity, with important consequences for the early universe [7, 8].

Given this situation, it is worth examining as carefully as possible the theoretical assumptions of the standard cosmological model, if for no other reason than to reassure ourselves that its apparent fine-tunings are not pointing toward a radically different underlying framework. In this paper we consider the empirical evidence relating to the Friedmann equation, the dynamical relation in general relativity between the expansion rate of the Universe and the energy density in it.

The fundamental quantity in general relativity is the space-time metric. We have some empirical evidence for the form of the metric from astronomical observations. We know that the Universe is expanding [9], i.e., the physical volume of the Universe is increasing with time. We also know that the cosmic microwave background is isotropic to a part in 10^5 [10]. Therefore, it seems reasonable to assume that the spatial metric is isotropic. If we further assume that all observers (matter) in this expanding isotropic Universe see the same CMB isotropy, then it follows [11] that the Universe is homogeneous (on scales much larger than that of the largest collapsed structure). The metric is then uniquely determined. The form of this metric, called the Robertson-Walker (RW) metric, is

$$ds^2 = -dt^2 + a^2(t) \left[\frac{dr^2}{1 - kr^2} + r^2 d\Omega^2 \right] , \quad (1)$$

where $a(t)$ is the scale factor and $k \in \{-1, 0, +1\}$ is the curvature parameter. The Fried-

mann equation (derived from general relativity for the RW metric) is

$$H^2 = \left(\frac{\dot{a}}{a}\right)^2 = \frac{8\pi G}{3}\rho - \frac{k}{a^2} . \quad (2)$$

$H = \dot{a}/a$ is the Hubble expansion rate and ρ the energy density of the universe. In fact (2) is only the 00 component of Einstein's equations applied to (1); we also have another independent gravitational equation,

$$\frac{\ddot{a}}{a} = -\frac{4\pi G}{3}(\rho + 3p) , \quad (3)$$

as well as an equation of energy-momentum conservation,

$$\dot{\rho} = -3(\rho + p)\frac{\dot{a}}{a} , \quad (4)$$

where p is the pressure. In seeking to test this framework, we might hope to seek consistency relations among these equations, which could be compared with data. Unfortunately, it is always possible to find an energy density $\rho(t)$ and pressure $p(t)$ which satisfy (2-4). Specifically, any given expansion history $a(t)$ and curvature k is compatible with these equations if we choose

$$\rho = \frac{3}{8\pi G} \left[\left(\frac{\dot{a}}{a}\right)^2 + \frac{k}{a^2} \right] \quad (5)$$

$$p = -\frac{1}{8\pi G} \left[2\frac{\ddot{a}}{a} + \left(\frac{\dot{a}}{a}\right)^2 + \frac{k}{a^2} \right] . \quad (6)$$

The crucial point here is that a perfectly smooth component of energy and pressure cannot be detected in any way except for its influence on the expansion rate, so we have no independent constraint on such a source. While invoking a perfectly smooth component to fit an arbitrary behavior of the scale factor might seem like cheating, this is exactly what we must do to reconcile the strong evidence in favor of spatial flatness with the similarly strong evidence that the amount of clustered matter falls far short of the critical density in the current universe. In this sense, the set of equations (2-4) are, strictly speaking, untestable, without some prior expectation for the nature of ρ and p .

Instead, we can characterize what observations can tell us about the behavior of the scale factor in a model-independent way, so that any specific alternative theory can be straightforwardly compared with the data. There are only two eras of the universe's history in which such a characterization is possible: the recent universe, and the BBN era. In the recent universe, information about the behavior of the scale factor can be obtained in a

variety of ways, most directly by comparing the distance of faraway objects to their redshifts, as is done in the supernova studies that first revealed the acceleration of the universe [1]. During BBN, the expansion rate directly affects the relative abundances of light elements produced (as reviewed below), so that the primordial abundances are a powerful constraint on alternative expansion histories.

Other important observable phenomena which are affected by the expansion rate do not offer such a direct test, since they typically involve the local behavior of gravity (evolution of perturbations) in addition to its cosmological behavior (evolution of the scale factor). Examples include the growth of large-scale structure and the imprinting of temperature anisotropies on the CMB. A theory which predicts deviations from the Friedmann equation could generically predict deviations from the predictions of general relativity on other scales. Consequently, it is difficult to use the growth of structure and CMB anisotropies as model-independent tests of the Friedmann equation, although any fully-specified alternative theory might be tightly constrained by these phenomena. However, if one assumes that the local behavior of gravity as predicted by general relativity is correct, then structure formation and CMB anisotropies are a powerful probe of the expansion history (and hence dark energy evolution) after the last scattering epoch [12].

In this paper we will study what kinds of expansion histories in the early universe are compatible with the BBN explanation of the light element abundances. Other works have constrained the energy density [13] or value of Newton's constant [14] during BBN, assuming the Friedmann equation, or have derived BBN constraints on specific scalar-tensor theories [15, 16] or have put limits on alternative cosmologies under the assumption that the universe has undergone a consistent power-law evolution from very early times [17]. An estimate of the constraints imposed by BBN (by considering the change in the neutron-proton freeze-out temperature) and structure formation on cosmologies where the energy density in the universe varies as some power of H has also been calculated [8]. Our approach will be not to assume any specific behavior of the scale factor over long periods, but instead to introduce a two-parameter family of evolution histories which we take to be valid only in the vicinity of BBN. We find that a variety of alternative cosmologies can be consistent with observations, although they comprise essentially a one-dimensional region in our two-dimensional space of possibilities.

2 Parameterizing the scale factor during BBN

We will consider theories in which the field equations for the metric may be different from those of general relativity, but we assume that test particles will still follow geodesics of this metric. From this assumption it follows that the energy of a relativistic particle redshifts as $1/a$. The photon temperature will be proportional to $1/a$ in the absence of entropy creation; however, e^\pm annihilation can act as a significant entropy source. We therefore use the neutrino temperature T as a measure of the scale factor, since $T \propto 1/a$ to excellent accuracy during the epoch under consideration. Of course these statements rely on our decision to only consider changes in the gravitational dynamics, not any particle-physics processes.

The process of conventional BBN spans temperatures between the freeze-out of weak interactions, $T_f = 1 \text{ MeV}$, and the synthesis of helium, $T_{\text{BBN}} = 60 \text{ keV}$; this corresponds to a change in the scale factor by slightly more than one order of magnitude. It will therefore be reasonable to approximate the expansion rate during this interval, so long as it is not wildly oscillating or somehow finely tuned, as a simple power law:

$$H(T) = \left(\frac{T}{1 \text{ MeV}} \right)^\alpha H_1 . \quad (7)$$

Any expansion history is parameterized by the coefficient H_1 and the exponent α . (One can view this as a Taylor expansion in $\log(H)$, to first order in $\log(T)$.) We do not extend this parameterization beyond the BBN epoch, nor are we proposing any models in which (7) is predicted (but note that all the models in [7, 8] are well described by this expansion law); this is a phenomenological study of the expansion rate during BBN. It should also be noted that there might exist models which are not accurately described by power-law expansion during the BBN era [16]; in such cases it would be necessary to examine each model individually.

In standard BBN weak interactions freeze out close to $T_f = 1 \text{ MeV}$, at which point $n/p(T_f) \approx 1/6$. At temperatures lower than T_f , the only change in the neutron to proton ratio occurs due to free decay of neutrons with a lifetime of $\tau_n = 887 \text{ sec}$. At temperatures much lower than freeze-out, it becomes possible to synthesize helium in appreciable quantities. This happens at a temperature of $T_{\text{BBN}} = 60 \text{ keV}$, and essentially all the remaining neutrons (one per seven protons) are bound into helium nuclei. It should be noted that this temperature (T_{BBN}) is much lower than the binding energies of all the light elements. Clearly, the large photon to baryon ratio (which implies a large photo-dissociating background) is partly responsible for this [18]. The rate at which $n \rightarrow {}^4\text{He}$ conversion occurs

depends on the destruction rate of deuterium which in turn depends on the binding energy of deuterium, the formation rate of tritium and the baryon to photon ratio. In standard BBN, it turns out that the conditions for helium synthesis are just right when the helium formation rate is larger than $1/\tau_n$ [19]. This picture breaks down in the unconventional expansion histories we consider.

An understanding of how alternative models affect light-element abundances can be expressed in terms of the behavior of three characteristic quantities: the freeze-out temperature T_f (which sets the initial neutron/proton ratio), the time interval between freeze-out and nucleosynthesis, $\Delta t_{\text{BBN}} = t_{\text{BBN}} - t_f$ (during which neutrons decay), and the Hubble parameter at nucleosynthesis, H_{BBN} (which affects the efficiency with which neutrons are converted to helium, and thus determines the deuterium and lithium abundances). Note that $\Delta t_{\text{BBN}} \approx t_{\text{BBN}}$, since $t_f \ll t_{\text{BBN}}$; this will continue to be true in the non-standard models we study. Assuming only that H is monotonically decreasing even prior to the epoch when this formula is relevant, we will have

$$t_{\text{BBN}} = \frac{1}{\alpha H_{\text{BBN}}} . \quad (8)$$

The predictions of Big-Bang nucleosynthesis are given as ratios of abundances of the light elements – neutrons (n), protons (p or H), deuterium (D), ^3H , ^3He , ^4He and ^7Li . One quotes the ratio of the number density of the light elements to the number of protons, except in the case of helium where the accepted practice is to quote its mass fraction (Y_P). The absolute density of these light elements is set by the absolute density of baryons. The only input parameter in standard BBN is the baryon density quoted as its ratio (η) to the number density of photons. It is useful to define $\eta_{10} = 10^{10}\eta$ since the number density of baryons (compared to that of photons) is very small. Except for a brief period when electrons and positrons annihilate, η remains constant (provided no other entropy changing interactions come into equilibrium).

We will adopt observationally allowed ranges of light elements ratios in keeping with the inferences (but slightly on the conservative side) of Olive *et al.* [20]. The ranges are $0.228 \leq Y_P \leq 0.248$, $2 \leq 10^5 \times D/H \leq 5$, and $1 \leq 10^{10} \times ^7\text{Li}/H \leq 3$. The low deuterium value has been adopted since it seems to be favored by current data [21].

The baryon density is not as well constrained observationally as the ratios of light element abundances. One reason for this is that we can only inventory the baryons that we see and most of the baryons could be dark. Even putting a lower bound on the baryon density is a difficult task. Persic and Salucci [22] estimated the density of baryons in the

Universe (in terms of η_{10}) to be $\eta_{10} \geq 0.3$. In converting the baryon density to η we have assumed that η has remained constant since BBN (as it does in the standard model), and that $H_0 \geq 60 \text{ km s}^{-1}$ [23] where H_0 is the present expansion rate of the Universe. Fukugita *et al.* [24] also did a baryon inventory and their bound on the baryon density translates to $\eta_{10} \geq 1.8$, a much higher lower bound on the baryon density. We will use both these lower bounds as a way of showing how the allowed region changes with the bound on the baryon density.

Without recourse to a specific theory of gravity it is not possible to put an upper bound on the baryon density. For our purposes, we will assume the following ranges for the baryon density – a tight bound corresponding to $1 \leq \eta_{10} \leq 10$ and a broader range with $0.5 \leq \eta_{10} \leq 50$. We will also comment on what happens if the upper bound on the baryon density is increased.

3 Helium constraints

The requirement that about 24% helium by mass be synthesized imposes severe constraints on the expansion history for temperatures around T_{BBN} . To understand these constraints, it proves useful to look at the effects of changes in the parameters H_1 and α of (7) in the vicinity of the standard model. We first concentrate on the effect of changing H_1 at fixed α . As mentioned, the important considerations are the freeze-out temperature T_f , and the time interval between freeze-out and nucleosynthesis $\Delta t_{\text{BBN}} \approx t_{\text{BBN}}$. (In the vicinity of standard BBN, small changes in the expansion rate H_{BBN} will not be important, since essentially all neutrons are converted to helium.) Increasing H_1 increases the expansion rate at every temperature; thus, freeze-out will occur earlier (T_f will be higher) leading to a larger initial neutron/proton ratio. At the same time, the faster expansion rate leads to a decrease in t_{BBN} , leaving less time for neutrons to decay. Both these effects go in the same direction and hence the neutron/proton ratio at T_{BBN} increases with increasing H_1 , leading to a higher helium abundance.

One can analyze the effect of changing α at fixed H_1 in a similar manner. Again, the relevant considerations in the vicinity of standard BBN are the behaviors of T_f and Δt_{BBN} . Since H_1 corresponds to a temperature close to freeze-out and before helium synthesis, increasing α means that the expansion rate will be lower during nucleosynthesis. In particular this implies that H_{BBN} will be lower (i.e., helium synthesis happens later), and hence that the time interval $\Delta t_{\text{BBN}} \propto 1/H_{\text{BBN}}$ will be longer. Consequently, increasing α at fixed H_1

gives neutrons more time to decay between T_f and T_{BBN} , working to decrease the helium abundance for values close to the standard ones.

We can therefore balance the effects of increasing H_1 against those of increasing α , to obtain a constant helium abundance for small deviations from the standard picture. In Figure 1 we plot contours of constant ${}^4\text{He}$ in the α - H_1 plane. This figure reveals the

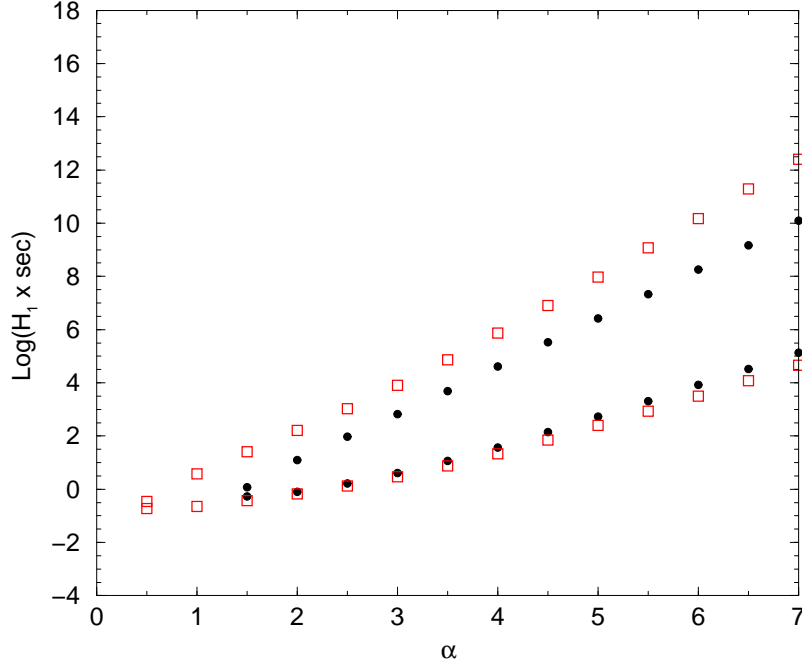


Figure 1: Contours representing constant helium in the α - H_1 plane, for $Y_P = 0.24$. We have chosen $\eta = 10^{-10}$ (filled circles) and $\eta = 10^{-9}$ (squares) for purposes of illustration.

expected behavior in the vicinity of the standard model, but we see that the curves turn over, and at fixed α there is a larger value of H_1 for which the helium abundance is the same. This feature has been previously noted in the context of exploring the effects of very large numbers of light neutrino species (and thus H_1) [25] and in the explorations of BBN constraints on scalar-tensor theories of gravity [26]. For very large H_1 , the freeze-out temperature is sufficiently high that $n/p(T_f)$ asymptotes to unity; Δt_{BBN} continues to decrease as H_1 increases, leading to an ever-larger neutron fraction at nucleosynthesis. However, H_{BBN} also increases and eventually the expansion rate at nucleosynthesis is so large that there is not enough time to efficiently turn the neutrons into helium. Thus, given the success of standard BBN, there will be an additional larger value of H_1 (at the standard value $\alpha = 2$) for which the helium abundance is the same. This argument can be generalized not just to other values of α but also to the other light element abundances.

One expects (at fixed α) to get two values of H_{BBN} which produce the same abundance.

4 Deuterium and Lithium constraints

The deuterium abundance provides an important additional constraint on the allowed parameter space. In the standard picture deuterium is a by-product of neutrons getting burnt to helium. Since the abundance of deuterium is set by its destruction rate and the time available for this destruction, it is extremely sensitive to the expansion rate at temperatures close to T_{BBN} . Around the standard model, D/H increases with H_1 for a fixed α , since the time available for nucleosynthesis decreases. If one fixes H_1 , the decrease in post-BBN ($T \lesssim T_{\text{BBN}}$) expansion rate causes D/H to decrease with increasing α . Once again we see that there is a trade-off to be made between α and H_1 , and hence it is possible to increase α and H_1 simultaneously such that we end up with the same deuterium abundance. This is borne out by the contours of constant deuterium plotted in Figure 2. Note that one expects exactly the opposite behavior with respect to changes in α (with H_1 fixed), and H_1 (with α fixed) for the upper branch of contour plot. Essentially, the abundances in the upper branch of the contour plot increase if the time available for nucleosynthesis goes up.

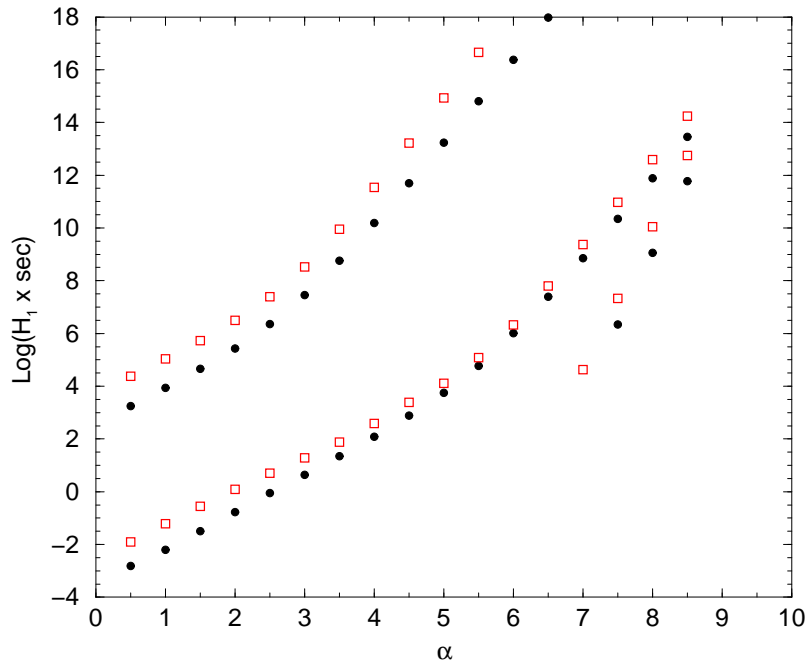


Figure 2: Contours of constant deuterium, $D/H = 3 \times 10^{-5}$, at $\eta = 10^{-10}$ (filled circles) and $\eta = 10^{-9}$ (squares).

From Figure 2 it is clear that the lower branch of the contour plot turns over at large α . This can be traced to the appearance of a new production channel. As α increases without a corresponding exponential increase in H_1 , the time available for nucleosynthesis becomes very large, and consequently deuterium is almost completely destroyed. In the lower branch this implies that beyond a certain value of α it would not be possible to produce a reasonable D/H abundance. However, if the age of the Universe gets large enough it becomes possible to produce deuterium by pp fusion, in a manner similar to what happens in the sun. This pp burning explains the turn over towards smaller values of H_1 in the lower branch of the deuterium contour. For this solution to work, the age during nucleosynthesis has to be of the order of billions of years. We, therefore, consider this solution highly unlikely and do not include it in our analysis.

For our parameter space around the standard model we expect the same behavior with respect to η as in standard BBN. All other things being the same, increasing η decreases deuterium abundance while increasing Y_P due to more efficient nucleosynthesis. Thus at fixed α if η is increased, then one needs to decrease H_1 to lower the helium abundance back to where it was. In the case of deuterium, if η is increased at fixed α , then one needs to increase H_1 in order to increase D/H back to where it was.

Note that for the upper branch one would have to increase H_1 at fixed α to compensate for an increase in η for *both* helium and deuterium, since both Y_P and D/H increase with η in the upper branch.

We can infer the primordial abundance of ${}^7\text{Li}$ very accurately from poor-metallicity stars [20]. Therefore, it provides an additional constraint on our parameter space. For most of the parameter space, getting helium right automatically ensures that lithium is near the observed abundance. Even so, with the very tight bounds on ${}^7\text{Li}/\text{H}$ that we impose, lithium does provide strong constraints. Figure 3 shows contours of constant lithium in the H_1 - α plane. Its behavior with respect to a change in η follows that of helium.

The ${}^7\text{Li}$ iso-abundance contour has two interesting features not present in the helium contour, which can be traced to the fact that ${}^7\text{Li}$ has two distinct production channels. ${}^7\text{Li}$ can be produced through the reaction ${}^4\text{He}({}^3\text{H},\gamma){}^7\text{Li}$, and through ${}^4\text{He}({}^3\text{He},\gamma){}^7\text{Be}$ with the subsequent beta-decay of ${}^7\text{Be}$. Fixing our attention on the lower branch of the lithium contour, as we move from low to high α , the dominant production channel changes from the direct ${}^7\text{Li}$ channel to the indirect ${}^7\text{Be}$ one. The kink in the lower branch of the contour is at values of α where this transition takes place. At large α and H_1 , there is a small closed contour below the upper branch. For a fixed α in the region spanning the width of

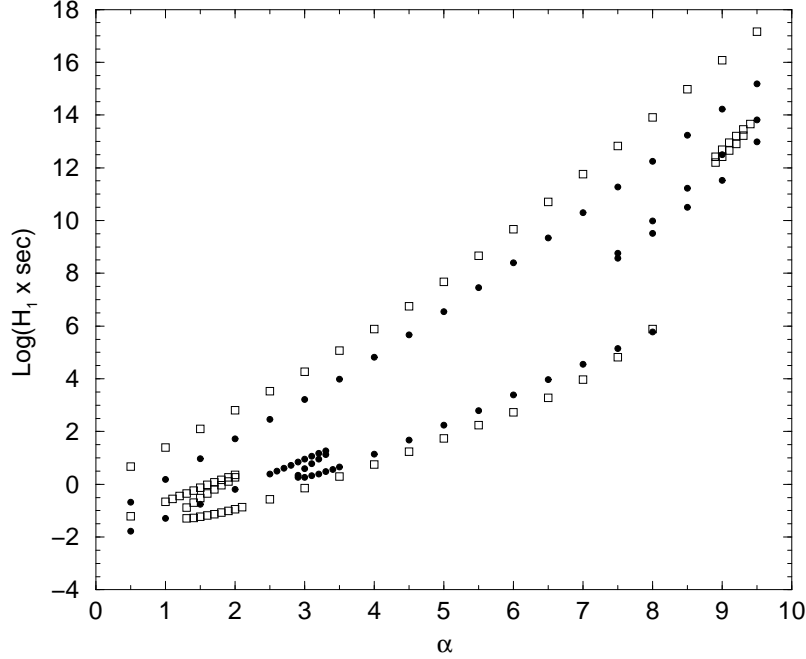


Figure 3: Contours of constant lithium, ${}^7\text{Li}/\text{H} = 3 \times 10^{-10}$, at $\eta = 10^{-10}$ (filled circles) and $\eta = 10^{-9}$ (squares).

the small closed contour, there are three values of H_1 which produce the required lithium abundance. The solution with the lowest value of H_1 produces ${}^7\text{Li}$ through the indirect ${}^7\text{Be}$ channel. In the upper branch of the contour ${}^7\text{Li}$ production is through the direct channel, for all values of α . A larger H_1 means shorter time for nucleosynthesis and since ${}^3\text{H}$ is easier to burn than ${}^3\text{He}$, the direct channel dominates.

5 Combined constraints

Putting together all of our constraints yields the allowed region shown in Figure 4. We note that the allowed region is essentially one dimensional, and is characterized by an almost linear relationship between $\log(H_1)$ and α . This tells us that there must exist a temperature T_c at which the expansion rate H_c is approximately fixed for all the models in the allowed range. In other words, we must have

$$H_1 = H_c (T_c / \text{MeV})^\alpha; \quad H_c = (0.039 \pm 0.013) / \text{sec} \quad \text{at} \quad T_c = 0.2 \text{ MeV}. \quad (9)$$

The range of H_c quoted in Eq. 9 corresponds to our conservative limits on the baryon to photon ratio. For the case with the tighter bound on baryon density, we obtain $H_c =$

$(0.03 \pm 0.004)/\text{sec}$. The value of T_c reflects of the physics involved. ${}^4\text{He}$ is primarily sensitive to H_1 (as well as to α), while the other elements (which can be viewed as by-products of the neutron to helium burning process) are mainly sensitive to H_{BBN} . Thus, not surprisingly, we have $1 \text{ MeV} > T_c > T_{\text{BBN}}$.

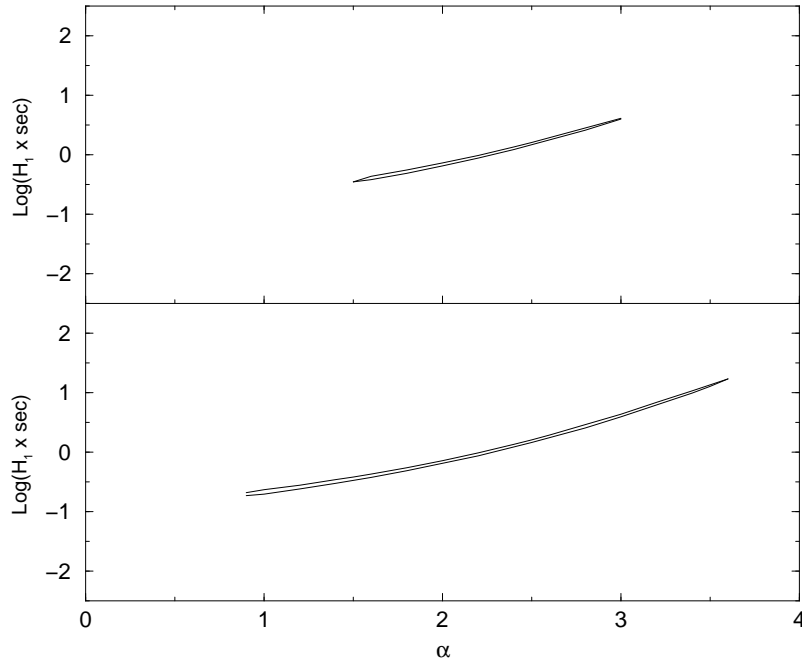


Figure 4: Allowed values of α and H_1 which lead to acceptable light element abundances. Upper panel shows the allowed parameter space when we constrain η_{10} to be between 1 and 10. The lower panel shows the allowed parameter space for $0.5 \leq \eta_{10} \leq 50$.

The coincidence that T_c is so close to the e^\pm annihilation temperature ($\simeq m_e/3 = 0.17 \text{ MeV}$) implies that the expansion rate of the Universe during e^\pm annihilation must have been close to the standard BBN value. This in turn implies that the cosmic microwave background will retain a black body spectrum through the annihilation epoch (as in standard BBN) in all the viable non-standard expansion histories we have identified.

The effect of a change in the assumed range of the baryon density on the bounds on α is visible in Figure 4. Decreasing the lower bound on η increases the upper bound on α , while allowing for larger baryon densities implies a smaller lower bound on α . The reason behind such behavior is not hard to understand. Given that the expansion rate at 0.2 MeV is approximately fixed, a viable expansion history with larger α has lower H_{BBN} . A lower H_{BBN} (i.e., more time for nucleosynthesis) at fixed baryon density implies a lower deuterium abundance. Thus one requires a smaller baryon density to get deuterium abundance right

in the limit of large α . Similarly, decreasing the lower bound on α requires larger baryon densities.

As discussed before, we do not really have an observational upper bound on the baryon density of the Universe in the absence of a theory of gravity. The lower bound is on a more sound footing because we can count the visible baryons. Thus it seems pertinent to ask what happens if one allows for larger cosmological baryon densities. From our arguments above we would expect viable models with smaller values of α . However, increasing η_{10} above 50 (panel 2 of Figure 4) has *no effect* on the allowed range of α . The reason behind this result is best understood through the following qualitative picture. At smaller values of α , and therefore larger H_{BBN} , one has a higher deuterium abundance if the baryon density is fixed. To lower the deuterium abundance to required levels one has to increase the baryon density. However, a larger baryon density (keeping α fixed) will lead to a larger helium fraction. Hence below a certain value of α (which depends on the constraints on the abundances) it is not possible to simultaneously obtain the correct amounts of deuterium and helium. This is also the reason why the allowed contour in the lower panel of Figure 4 does not appear to close.

6 Neutrino asymmetry

One of parameters in cosmology on which we have little handle is the neutrino asymmetry, i.e., the excess of neutrinos over anti-neutrinos or vice versa. This excess or deficit can be quantified by the neutrino chemical potential, μ , which enters into the Fermi-Dirac distribution function, given by $1/[1 + \exp(p/T + \mu/T)]$. The chemical potential of anti-neutrinos is $-\mu$. The ratio μ/T is an invariant, as long as there are no entropy-changing processes which involve neutrinos.

There are no compelling experimental or theoretical reasons to expect the neutrino (lepton) asymmetry ($\propto (\pi^2 + \mu^2/T^2)\mu/T$) to be orders of magnitude different from the baryon asymmetry. In fact, one might very well argue that it would only be natural for the baryon and lepton asymmetries to be comparable if they were formed by the same processes. However, we have no concrete experimental hints to back up our theoretical prejudice. Moreover, in our framework, the value of μ/T is virtually unconstrained (but for BBN) since the standard cosmological bounds [27] do not apply. Note that in order to probe $\mu/T \sim 1$ regime, one would require experiments which are capable of measuring neutrino energies down to 10^{-3} eV. As we shall shortly see, BBN even without the assumption of

standard gravity provides us with constraints on the value of the electron neutrino chemical potential in the $|\mu/T| = \mathcal{O}(1)$ regime.

Changing the neutrino chemical potential affects the neutrino number density. In standard BBN, a change in the neutrino number density affects the expansion rate and hence the abundances. Clearly, this effect is non-existent in our study. The electron neutrino chemical potential also affects the $n \leftrightarrow p$ reaction rates. This is the effect we shall be concerned with in this section. From here on, μ/T will implicitly refer to the electron neutrino chemical potential.

Detailed calculations of the effect of non-negligible μ/T (i.e., $|\mu/T| \gtrsim 1$) on BBN have been performed [28]. The salient points are (1) the equilibrium value of n/p is modified by a factor of $\exp(-\mu/T)$ from that when $\mu = 0$, (2) the neutrino decoupling and n - p freeze-out temperatures are changed. The first point clearly implies the constraint, $\mu/T < 2$, if a helium-4 mass fraction of 24% is to be synthesized. In Figure 5 we plot the allowed contours in $\alpha - H_1$ plane. The contours are labelled by the value of μ/T . We have restricted Y_P to being 24.4%. Allowing for our previously adopted range in Y_P will not change the result much as is apparent from the fact that the allowed contours in Figure 4 are practically 1-dimensional. We note that if α is set equal to 2, then we are back to standard cosmology; Figure 5 then provides us with the constraint on the number of relativistic degrees of freedom ($\propto H_1$) [28].

The principal feature in Figure 5 is the trend of the required value of H_1 being larger for larger μ/T . At larger μ/T , the equilibrium value of n/p is smaller, and hence to compensate for that t_{BBN} must be smaller or H_1 larger. For $\mu/T < -10$ no solutions were found, which owes to the fact that at the small values of H_1 required to produce the right helium-4, t_{BBN} gets so large that one cannot synthesize acceptable amounts of D/H .

7 Discussion

We have shown that the viable (i.e., satisfying BBN abundance constraints) expansion histories can be well approximated by the range of allowed values of α , for a fixed value of μ/T . Lets concentrate on the more “natural” $|\mu/T| \ll 1$ (equivalent to $\mu = 0$) case. Given the allowed range of α one can generate the allowed range of expansion rates at any temperature from about an MeV to 50 keV by using

$$H(T) = H_c (T/T_c)^\alpha . \quad (10)$$

We have plotted the history of these viable non-standard Universes in Figure 6.

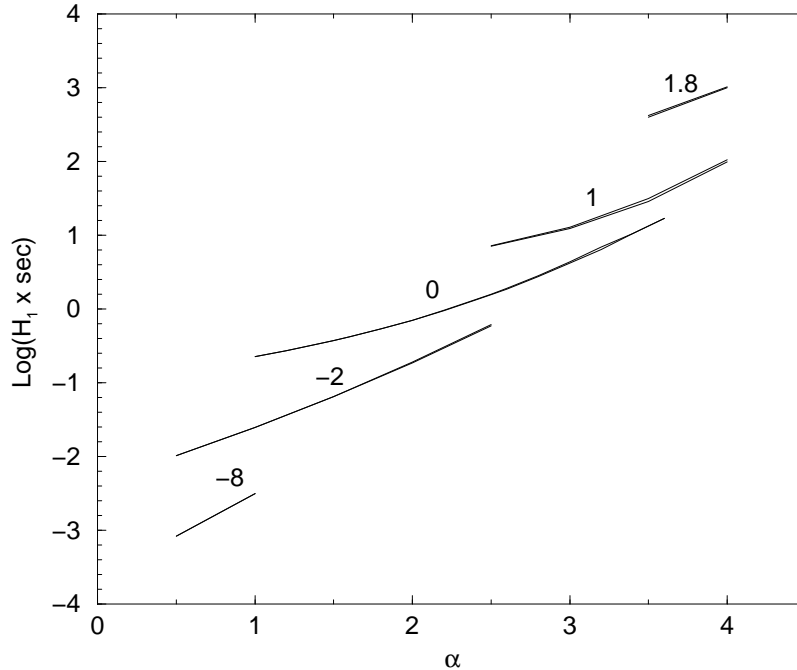


Figure 5: Allowed values of α and H_1 for $Y_P = 0.244$ and $0.5 \leq \eta_{10} \leq 50$. The contours are labelled by the value of μ/T . No solutions consistent with our constraints were obtained for $\mu/T > 2$ and $\mu/T < -10$.

The most interesting result of our study is that there is a range of expansion histories that are compatible with the observed light-element abundances. There is therefore room for substantial deviation from the standard cosmological model at early times, while remaining consistent with empirical evidence. On the other hand, it is encouraging to note that our allowed region (essentially one-dimensional) is only a small volume of the entire parameter space. In this sense it would be unlikely to find that any particular model was both very different from the standard picture, and consistent with the data.

We have also considered the effect of a large neutrino chemical potential. Independent of general relativity, BBN constrains the value of the electron neutrino chemical potential to $-10 < \mu/T < 2$. Of course, this increases the allowed range of H_1 considerably, as can be gauged from Figure 5.

Throughout this discussion we have assumed tight but reasonable bounds [20] on the light element abundances. Our quantitative results are sensitive to the assumed ranges. As observations improve further, it will be possible to precisely pin down the expansion history of the Universe during the epoch of nucleosynthesis.

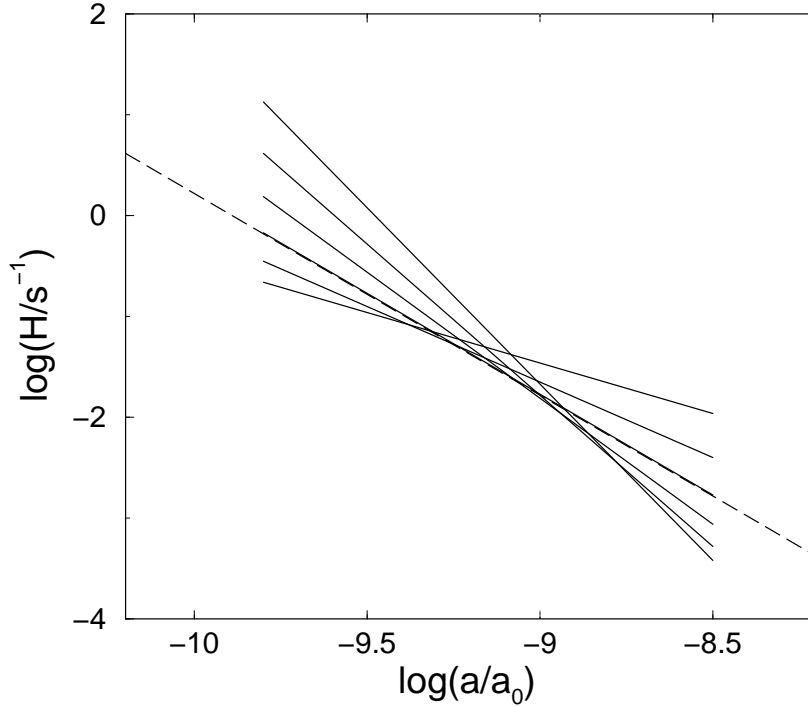


Figure 6: The expansion rate H as a function of scale factor a , for the family of allowed models in our parameterization (corresponding to our conservative limits on the baryon/photon ratio and negligible electron neutrino asymmetry). The dashed curve represents the standard model, and the solid curves are different allowed histories. It is clear that there is a value of the scale factor $a_c/a_0 \simeq 8.5 \times 10^{-10}$ at which the allowed range in H is minimized; this corresponds to a temperature $T_c \simeq 0.2$ MeV.

Acknowledgments

We would like to thank Lloyd Knox and Michael Turner for useful conversations. This work is supported in part by the Alfred P. Sloan Foundation, the David and Lucile Packard Foundation, and the U.S. Department of Energy.

References

- [1] A.G. Riess *et al.*, *Astron. J.* **116** (1998) 1009; S. Perlmutter *et al.*, *Astrophys. J.* **517** (1999) 565.
- [2] J.A. Peacock *et al.*, *Nature* **410** (2001) 169.

- [3] R. Stompor *et al.*, astro-ph/0105062 (2001); C. Pryke *et al.*, astro-ph/0104490 (2001); C.B. Netterfield *et al.*, astro-ph/0104460 (2001).
- [4] S. Burles, K.M. Nollett & M.S. Turner, Astrophys. J. Lett. **552**, L1 (2001) [astro-ph/0010171].
- [5] S. M. Carroll, Living Rev. Rel. **4**, 1 (2001) [astro-ph/0004075].
- [6] de Blok *et al.*, Astrophys. J. **552** (2001) L23.
- [7] P. Binetruy, C. Deffayet & D. Langlois, Nucl. Phys. B **565**, 269 (2000) [hep-th/9905012]; C. Csaki, M. Graesser, C. Kolda & J. Terning, Phys. Lett. B **462**, 34 (1999) [hep-ph/9906513]; J. M. Cline, C. Grojean & G. Servant, Phys. Rev. Lett. **83**, 4245 (1999) [hep-ph/9906523]; P. Binétruy, C. Deffayet, U. Ellwanger & D. Langlois, Phys. Lett. **B477**, 285 (2000) [hep-th/9910219]; P. Kraus, JHEP 9912, 011 (1999) [hep-th/9910149]; T. Shiromizu, K. Maeda & M. Sasaki, Phys. Rev. D **62**, 024012 (2000) [gr-qc/9910076]; E. Flanagan, S. Tye & I. Wasserman, Phys. Rev. D **62**, 044039 (2000) [hep-th/9910498]; S. M. Carroll & L. Mersini, hep-th/0105007.
- [8] D.J.H. Chung & K. Freese, Phys. Rev. D **61** (2000) 023511 [hep-ph/9906542];
- [9] E. Hubble, Proc. Nat. Acad. Sciences **15**, 168 (1929).
- [10] G.F. Smoot *et al.*, Astrophys. J. **371**, L1 (1991).
- [11] J. Ehlers, P. Geren & R.K. Sachs, J. Math. Phys. **9**, 1344 (1964).
- [12] M. Tegmark, astro-ph/0101354.
- [13] P. Kernan & L.M. Krauss, Phys. Rev. Lett. **72**, 3309 (1994) [astro-ph/9402010]; T.P. Walker *et al.*, Astrophys. J. **376**, 51 (1991).
- [14] E.W. Kolb, M.J. Perry & T.P. Walker, Phys. Rev. D **86**, 869 (1986).
- [15] D. I. Santiago, D. Kalligas and R. V. Wagoner, Phys. Rev. D **56**, 7627 (1997) [gr-qc/9706017].
- [16] T. Damour and B. Pichon, Phys. Rev. D **59**, 123502 (1999) [astro-ph/9807176].
- [17] M. Kaplinghat, G. Steigman & T.P. Walker, Phys. Rev. D **61**, 103507 (2000) [astro-ph/9911066].

- [18] E.W. Kolb & M.S. Turner, *The Early Universe*, (Addison-Wesley, Redwood City, CA, 1990), Ch. 4.
- [19] R. Esmailzadeh, G.D. Starkman & S. Dimopoulos, *Astrophys. J.* **378**, 504 (1991)
- [20] K.A. Olive, G. Steigman & T.P. Walker, *Physics Reports* **333**, 389 (2000) [astro-ph/9905320].
- [21] D. Kirkman *et al.*, astro-ph/0103305.
- [22] M. Persic & P. Salucci, *Mon. Not. R. astron. Soc.* **258**, 14p (1992).
- [23] W.L. Freedman *et al.*, *Astrophys. J.* **553**, 47 (2001).
- [24] M. Fukugita, C.J. Hogan & P.J.E. Peebles, *Astrophys. J.* **503**, 518 (1998) [astro-ph/9712020].
- [25] K.A. Olive, D.N. Schramm, G. Steigman, M.S. Turner, & J. Yang, *Astrophys. J.* **246**, 557 (1981).
- [26] P.J.E. Peebles, *Astrophys. J.* **147**, 859 (1967).
- [27] K. Freese, E.W. Kolb & M.S. Turner, *Phys. Rev. D* **27**, 1689 (1983).
- [28] H. Kang & G. Steigman, *Nucl. Phys.* **B372**, 494 (1992).